fluids

MDPI

Article

A New Exact Solution for the Flow of a Fluid through Porous Media for a Variety of Boundary Conditions

U. S. Mahabaleshwar [1], P. N. Vinay Kumar [2,*], K. R. Nagaraju [3], Gabriella Bognár [4] and S. N. Ravichandra Nayakar [5]

[1] Department of Mathematics, Davangere University, Shivagangothri, Davangere 577 007, India
[2] Department of Mathematics, SHDD Government First Grade College, Paduvalahippe, Hassan 573 211, India
[3] Department of Mathematics, Government Engineering College, Hassan 573 201, India
[4] Faculty of Mechanical Engineering and Informatics, Institute of Machine and Product Design, University of Miskolc, 3515 Miskolc-Egyetemvaros, Hungary
[5] Department of Mathematics, University BDT College of Engineering, Davangere 577 004, India
* Correspondence: vinaykumarpn1981@gmail.com

Received: 23 May 2019; Accepted: 29 June 2019; Published: 8 July 2019

check for updates

Abstract: The viscous fluid flow past a semi-infinite porous solid, which is proportionally sheared at one boundary with the possibility of the fluid slipping according to Navier's slip or second order slip, is considered here. Such an assumption takes into consideration several of the boundary conditions used in the literature, and is a generalization of them. Upon introducing a similarity transformation, the governing equations for the problem under consideration reduces to a system of nonlinear partial differential equations. Interestingly, we were able to obtain an exact analytical solution for the velocity, though the equation is nonlinear. The flow through the porous solid is assumed to obey the Brinkman equation, and is considered relevant to several applications.

Keywords: Brinkman equation; viscosity ratio; first- and second-order slip; similarity transformation; porous medium

1. Introduction

The flow of a fluid through a porous medium has numerous applications in industries dealing with polymer extrusion process, glass blowing, metallurgical processes, and geophysical and allied areas (see [1]). A variety of equations have been used to describe the flow of a fluid through a porous medium as it is one of the important key factors in maintaining the temperature in the medium. These equations due to [2–5] and others, are merely approximations to the appropriate balance laws. A variety of ideas have been suggested to model the flow of mixtures, and one such approach is that which follows from the seminal works of Darcy and Brinkman and has been given a formal structure by [6,7]. Several specific problems have been solved using such an approach (see [8–19]). Here, we study the flow of a fluid through a porous media that is governed by the Brinkman equation (see [20–30]) for a discussion of the status of the Brinkman equation within the context of mixture theory). The fact that we are able to obtain an analytical solution to the problem makes the study all the more interesting. Despite the fact that advanced computing facilities are available to obtain the numerical solution, investigators around the world are much more interested in providing the analytical solution due to their accuracy, relevance, and convenient to analyze physical process, in comparison to numerical solutions. The analytical solution can provide a better assessment of consistency and parameter estimates. Many authors have investigated the fluid flow through porous media and provided analytical solution (see [31–37]). The novelty of this study is our use of a variety of boundary conditions that subsumes those that have been considered earlier, in addition to new conditions concerning slip and proportional shearing at the boundary.

In this study, we consider the flow of a fluid through a semi-infinite porous media with one boundary subject to the slipping or adherence of the fluid, the solid being proportionally sheared, and the fluid being injected at the boundary (see Figure 1). We are able to obtain an analytical solution by introducing a similarity variable that greatly simplifies the governing equation. The effects of the boundary conditions on the flow through the porous media are determined.

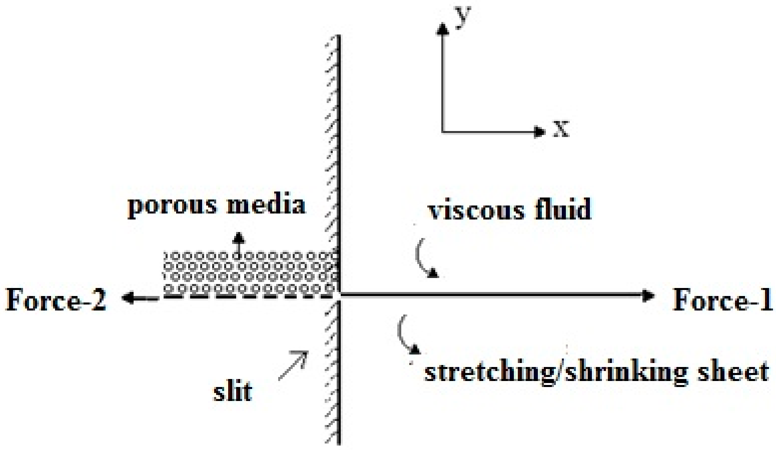

Figure 1. Schematic diagram showing stretching or contraction at the boundary.

2. Theoretical Model

Two dimensional laminar, steady, incompressible fluid flow through a porous media is considered. The x-axis is taken along the stretching of the sheet in the direction of the motion, and y-axis is perpendicular to the slit. In order to confine the fluid flow in the region $y > 0$, two forces of equal strength are applied along the x-axis. u and v denote the axial as well as transverse velocities in the flow field. Figure 1 depicts the physical flow problem subjected to the boundary conditions.

We considered the flow of the classical incompressible Navier-Stokes [38] fluid through a porous half-space. We assumed that the equations governing the flow are those given by the Brinkman equation for flow through porous media which assumes that the fluid is incompressible and, hence, the conservation of mass reduces to

$$\nabla \cdot \vec{q} = 0, \tag{1}$$

and the conservation of linear momentum that takes the form

$$\rho\left[\frac{1}{\phi}\vec{q}_t + \frac{1}{\phi}\left(\vec{q}\cdot\nabla\right)\vec{q}\right] = -\nabla p + \mu_{eff}\,\nabla^2\vec{q} - \frac{\mu}{K}\vec{q}, \tag{2}$$

where μ_{eff} represents the effective viscosity of the fluid(see [39,40]) provides the definition of the other parameters. The Brinkman equation can be shown to be obtained as a systematic approximation using mixture theory by assuming special structures for the interaction forces between the porous solid and fluid, and assuming the porous solid is rigid (see [41] for a detailed derivation).The transformed governing equations for the conservation of mass and the balance of linear momentum are given as

$$\frac{\partial u}{\partial x} + \frac{\partial v}{\partial y} = 0, \tag{3}$$

$$u\frac{\partial u}{\partial x} + v\frac{\partial u}{\partial y} = -\frac{\phi^2}{\rho_f}\frac{\partial p}{\partial x} + \phi^2 \nu_{eff}\frac{\partial^2 u}{\partial y^2} - \frac{\nu\phi^2}{K}u, \tag{4}$$

where $\nu = \frac{\mu}{\rho_f}$ and $\nu_{eff} = \frac{\mu_{eff}}{\rho_f}$. The Forchheimer term in the interaction is neglected as it produces little impact on the fluid flow in a porous medium governed by the Brinkman equation (see [42]). Also, the pressure gradient is neglected, and the time factor is zero for the steady case.

The governing boundary conditions are (see [43,44])

$$u(x,y) = d\alpha x + A\frac{\partial u}{\partial y} + B\frac{\partial^2 u}{\partial y^2}, \qquad \mathrm{v} = \mathrm{v}_c, \qquad \text{at} \qquad y = 0, \tag{5a}$$

$$u(x,y) \to 0, \qquad \text{as} \qquad y \to \infty. \tag{5b}$$

Here, d is the parameter of proportional shearing at the boundary, with $d \neq 0$ and $d = 0$ corresponding to the boundary at $y = 0$ and being either proportionally sheared or being fixed. The constants A and B represent the first- and second-order slip coefficients, respectively. Also, the mass transpiration parameter, v_c, represents suction or injection depending on $\mathrm{v}_c > 0$ or $\mathrm{v}_c < 0$, respectively.

In order to carry out the analysis, the physical stream functions in terms of similarity variables f and η are introduced as follows:

$$\psi = \sqrt{\alpha \nu_{eff}} \quad x f(\eta), \tag{6}$$

where

$$\eta = \frac{1}{\phi}\sqrt{\frac{\alpha}{\nu_{eff}}}\, y. \tag{7}$$

In terms of physical stream function ψ, the axial and transverse velocities can be rewritten as follows:

$$u = \frac{\partial \psi}{\partial y}, \quad \mathrm{v} = -\frac{\partial \psi}{\partial x}. \tag{8}$$

The Equation (8) satisfies the continuity equation. Upon substitution of Equations (6) and (7) into Equation (4), we obtain

$$\Lambda\frac{\partial^3 \psi}{\partial y^3} + \frac{\partial(\psi, \frac{\partial \psi}{\partial y})}{\partial(x,y)} - K_1\frac{\partial \psi}{\partial y} = 0. \tag{9}$$

Here, the second term indicates the Jacobian and subject. The appropriate boundary conditions are (see [43,44]) as follows:

$$\frac{\partial \psi}{\partial y} = d\alpha x + A\frac{\partial u}{\partial y} + B\frac{\partial^2 u}{\partial y^2}, \quad \frac{\partial \psi}{\partial x} = v_c \text{ at } \mathrm{y} = 0, \tag{10a}$$

$$\frac{\partial \psi}{\partial y} = 0, \qquad \text{as} \qquad \mathrm{y} \to \infty. \tag{10b}$$

Here, $\Lambda = \frac{\mu_{eff}}{\mu}$ is the Brinkman number or viscosity ratio. Using Equations (9) and (10) with Equation (6), the following transformed equation with constant coefficient is derived:

$$\Lambda f_{\eta\eta\eta} + f f_{\eta\eta} - f_\eta^2 - K_1 f_\eta = 0. \tag{11}$$

The governing boundary conditions for Equation (11) are given as

$$f(0) = V_c, \quad f_\eta(0) = d + \Gamma_1 f_{\eta\eta}(0) + \Gamma_2 f_{\eta\eta\eta}(0), \quad \text{at } \eta = 0, \tag{12}$$

$$f_\eta(\infty) \to 0 \quad \text{as } \eta \to \infty, \tag{13}$$

where $\Gamma_1 = A\sqrt{\frac{\alpha}{\nu}} > 0$ and $\Gamma_2 = B\frac{\alpha}{\nu} < 0$ are the first- and second-order slip parameters, and $K_1 = \frac{\nu\phi^2}{\alpha K}$ is the reciprocal of Darcy number $Da = \frac{l^2}{K}$, with $l = \phi\sqrt{\frac{\nu}{\alpha}}$ and $V_c = \frac{v_c}{\sqrt{\alpha\rho}}$ as the mass suction/injection parameters. The subscript denotes the derivative with respect to η.

3. The Analytical Solution

The flow problem considered is the generalization of the classical works of [43–48]. In our problem, the viscous flow with first- and second-order velocity slips over a porous half-space that is stretched or contracted at the boundary (see Figure 1), and the flow being governed by the Darcy–Brinkman model is considered. One obtains nonlinear partial differentiation from Equations (3) and (4), which are mapped into systems of the nonlinear ordinary differential Equation (11), with a constant coefficient by means of similarity transformation subjected to the imposed boundary (12)–(13).The analytical solution for the velocity distribution is determined.

The exact analytical solution of Equation (11) subjected to the governing boundary conditions Equations (12) and (13) is derived. The condition in Equation (13) suggests choosing the equation of the form

$$f(\eta) = A_1 + B_1\exp(-\beta\eta), \tag{14}$$

where $\beta > 0$ is to be determined later. Also, A_1 and B_1 are constants that are to be determined by using Equation (12):

$$A_1 = V_c + d\left(\frac{1}{\beta + \Gamma_1\beta^2 - \Gamma_2\beta^3}\right) \text{ and } B_1 = -d\left(\frac{1}{\beta + \Gamma_1\beta^2 - \Gamma_2\beta^3}\right). \tag{15}$$

It follows from Equation (11), (14), and (15) that

$$\Lambda\Gamma_2\beta^4 - (\Lambda\Gamma_1 + V_c\Gamma_2)\beta^3 + (V_c\Gamma_1 - \Lambda - K_1\Gamma_2)\beta^2 + (V_c + K_1\Gamma_1)\beta - (d + K_1) = 0. \tag{16}$$

Here, $\beta > 0$ is one of the real roots (see [49,50]).

By using the transformation variable $\xi = \beta + \frac{a_3}{4}$, Equation (16) transforms into

$$\xi^4 + p\,\xi^2 + q\,\xi + r = 0, \tag{17}$$

where $p = a_2 - \frac{3}{8}a_3^2$, $q = \left(A_1 - \frac{1}{2}A_2A_3 + \frac{1}{8}A_3^3\right)$, and $r = a_0 - \frac{1}{4}a_1a_3 + \frac{1}{16}a_2a_3^2 - \frac{3}{256}a_3^4$, and $a_3 = -\frac{\Lambda\Gamma_1 + V_c\Gamma_2}{\Lambda\Gamma_2}$, $a_2 = \frac{V_c\Gamma_1 - \Lambda - K_1\Gamma_2}{\Lambda\Gamma_2}$, $a_1 = \frac{V_c + K_1\Gamma_1}{\Lambda\Gamma_2}$, $a_0 = \frac{d + K_1}{\Lambda\Gamma_2}$.

The four corresponding roots of the algebraic Equation (17) are

$$\beta_1 = \frac{\sqrt{C}}{2} + \frac{1}{2}\sqrt{D_1} - \frac{a_3}{4}, \tag{18a}$$

$$\beta_2 = \frac{\sqrt{C}}{2} - \frac{1}{2}\sqrt{D_1} - \frac{a_3}{4}, \tag{18b}$$

$$\beta_3 = -\frac{\sqrt{C}}{2} + \frac{1}{2}\sqrt{D_1} - \frac{a_3}{4}, \tag{18c}$$

$$\beta_4 = -\frac{\sqrt{C}}{2} - \frac{1}{2}\sqrt{D_1} - \frac{a_3}{4}, \tag{18d}$$

where

$$D_1 = D - \frac{2q}{C},$$

$$C = -\frac{2p}{3} + 2^{1/3}\left(p^2 + 12r\right)\left[3\left(2p^3 + 27q^2 - 72pr + \sqrt{-4\left(p^2 + 12r\right)^3 + \left(2p^3 + 27q^2 - 72pr\right)^2}\right)^{1/3}\right]^{-1}$$
$$+\left(2^{1/3}\,3\right)^{-1}\left(2p^3 + 27q^2 - 72pr + \sqrt{-4\left(p^2 + 12r\right)^3 + \left(2p^3 + 27q^2 - 72pr\right)^2}\right)^{1/3}$$

and

$$D = -\frac{4p}{3} - 2^{1/3}\left(p^2+12r\right)\left[3\left(2p^3+27q^2-72pr-\sqrt{-4\left(p^2+12r\right)^3+\left(2p^3+27q^2-72pr\right)^2}\right)^{1/3}\right]^{-1}$$
$$-\left(2^{1/3}\,3\right)^{-1}\left(2p^3+27q^2-72pr+\sqrt{-4\left(p^2+12r\right)^3+\left(2p^3+27q^2-72pr\right)^2}\right)^{1/3}$$

Equation (18) gives the complete solution of Equation (17). However, it should be noted that there is only one feasible solution for the Equation (17) when $\Gamma_2 < 0$, and based on the flow field Equation (16) has feasible solutions for $\beta > 0$.

4. Results and Discussion

In this paper, we were able to establish the impact of various physical parameters on the velocity distribution. The solutions obtained are in good agreement with that of the classical works when suitably restricted to specific conditions. The main emphasis of this study is the effect of boundary conditions on the flow through porous media. There are several possibilities at the boundaries, namely, the fluid meeting the no-slip adherence condition, the Navier slip condition, the second-order slip condition, as well as the possibility of blowing of the fluid.

The effects of physical parameters such as the mass transpiration parameter (V_C), first-order Navier slip (Γ_1), second-order slip (Γ_2),Brinkman ratio (Λ), and proportional shearing parameter (K_1)are discussed graphically. As the velocity distribution is an exponential function with a negative argument, it decreases with the increase in η. Since β is a function of mass transpiration parameter (V_C), first-order Navier slip (Γ_1), second-order slip (Γ_2), Brinkman ratio (Λ), and proportional shearing parameter (K_1)both axial as well as transverse velocities are forced to decrease exponentially.

The solution domain of β in Equation (16)has only complex roots when $D_1 < 0$, only real roots when $D_1 > 0$,and real repeated roots when $D_1 = 0$. Figure 2a–d depicts the solution behavior of β verses V_C for various values of D_1 and Γ_1. Figure 3a–d depicts the solution domain of β versus V_C for different values of K_1. In fact, by choosing $\Gamma_2 = 0$, Equation (16) reduces to a cubic equation and with the proper choice of Γ_1, Λ, and K_1, and the results are reduced to those obtained by [43,51,52].

Figure 4a–c demonstrates the impact of first-order velocity slip with proportional shearing on the solution domain of β versus V_c. The presence of a larger slip drags the separation curve towards the slit. The viscous fluid flow in a permeable medium with slip in a stretching boundary is quite different from that of a contracting boundary.

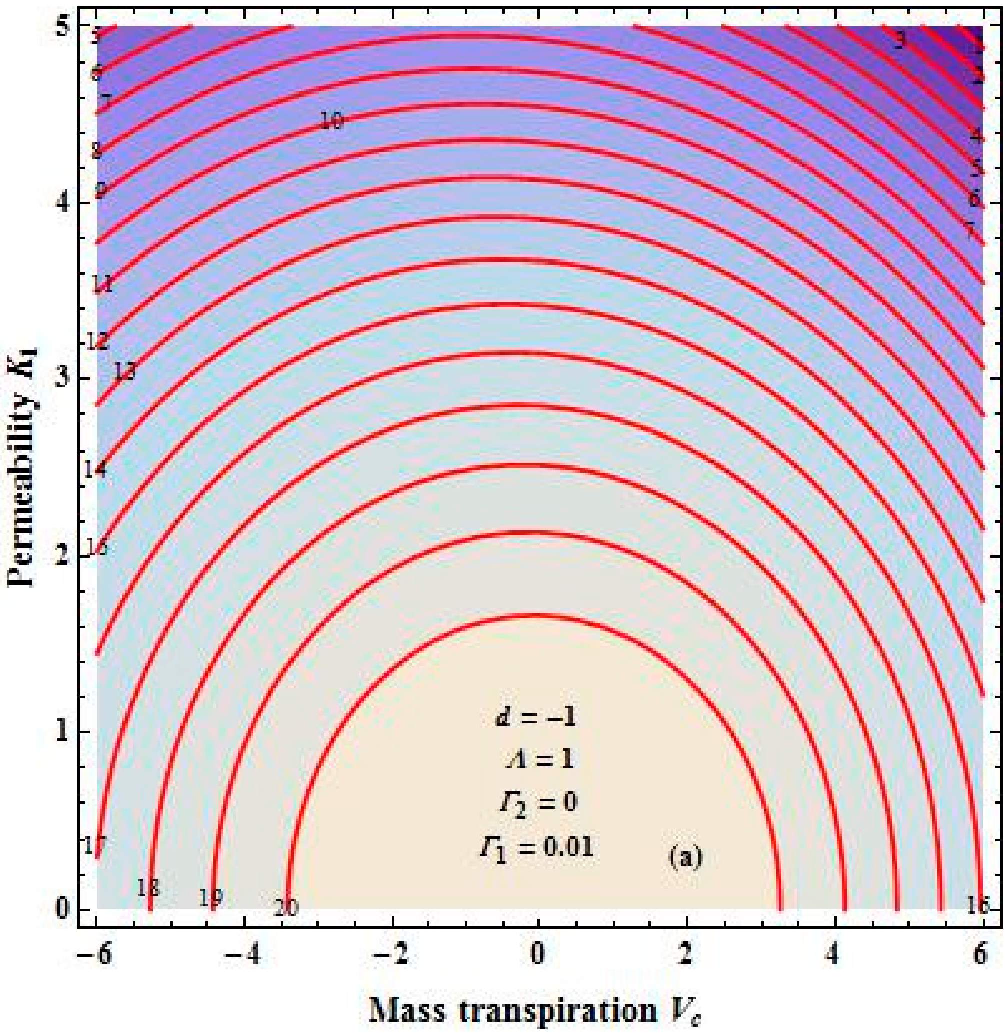

Figure 2. *Cont*.

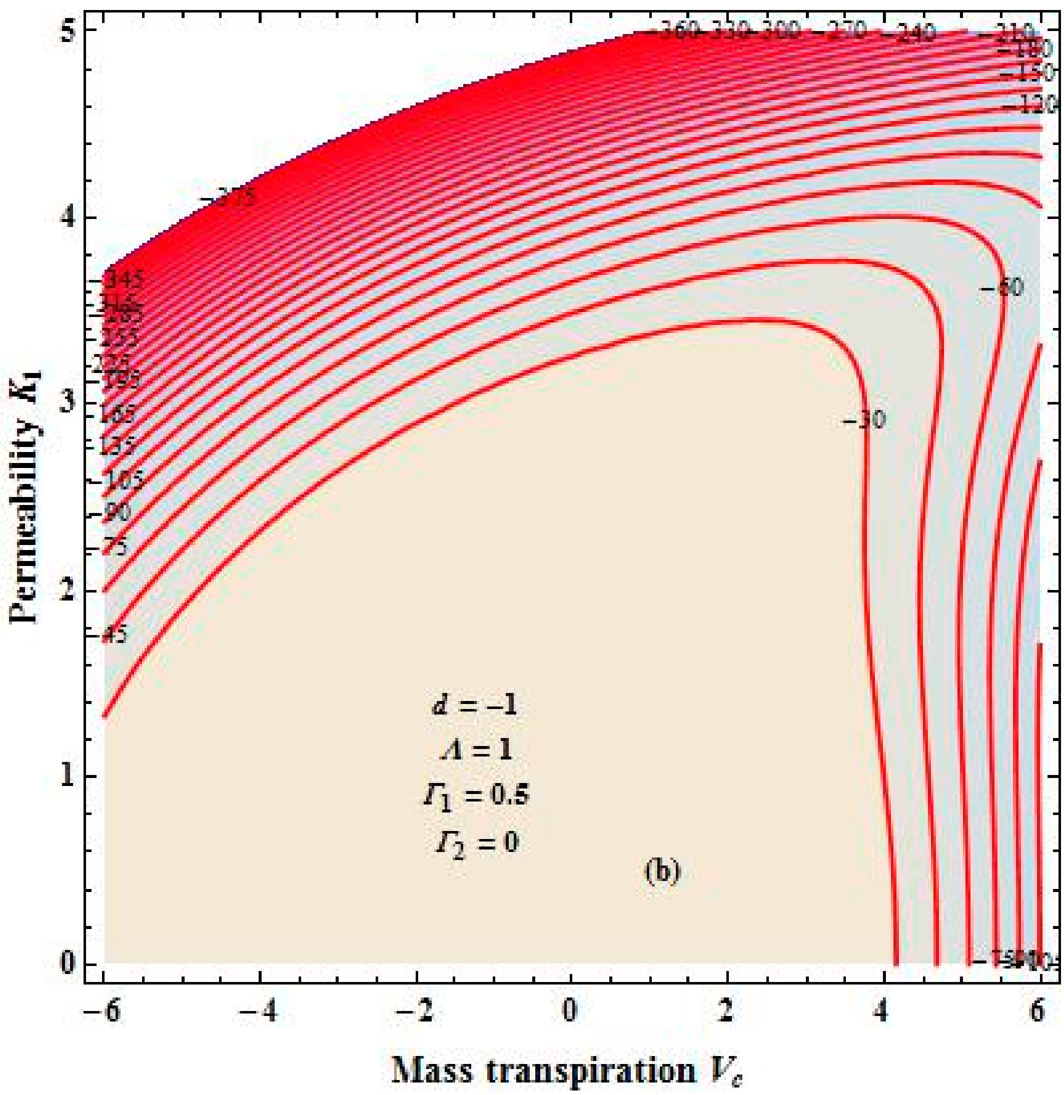

Figure 2. *Cont*.

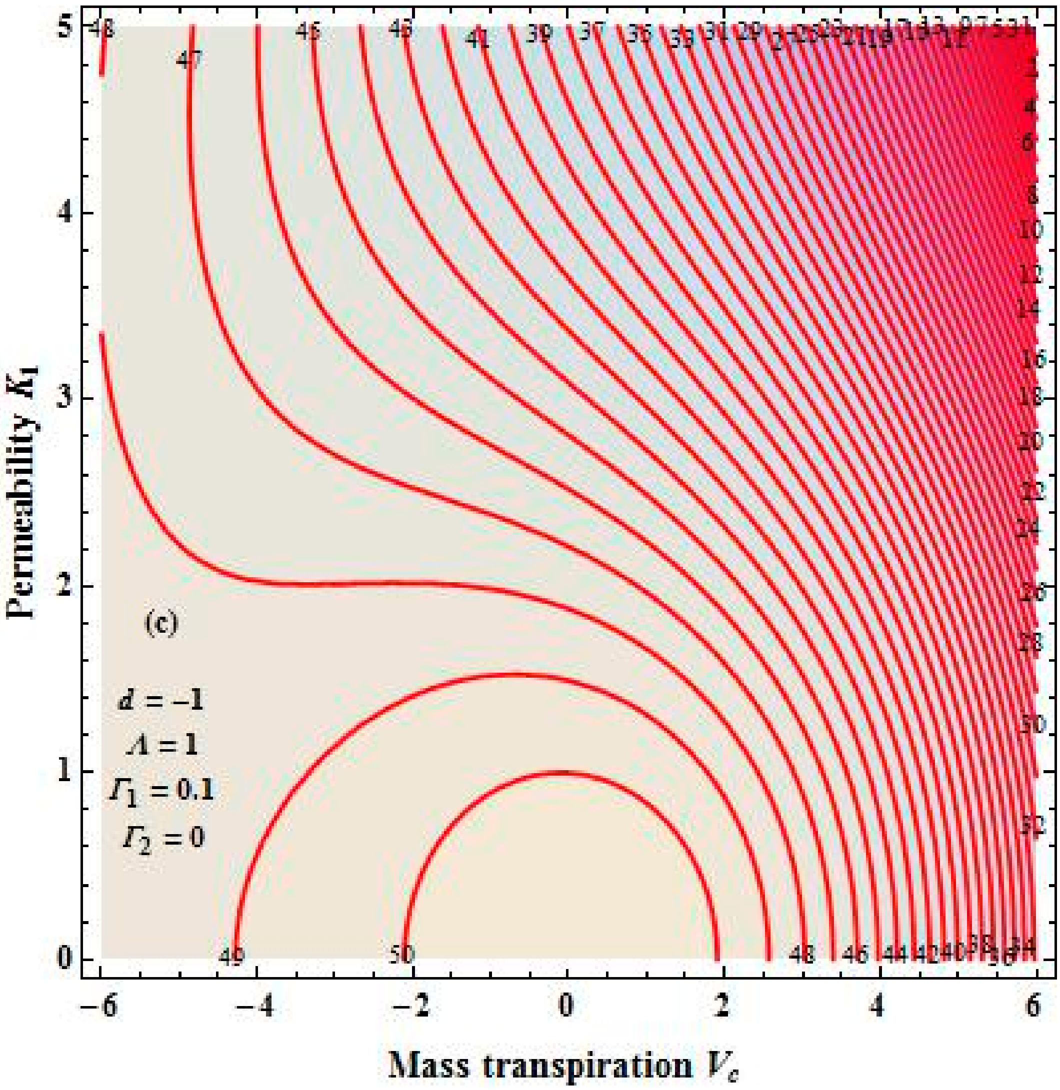

Figure 2. *Cont*.

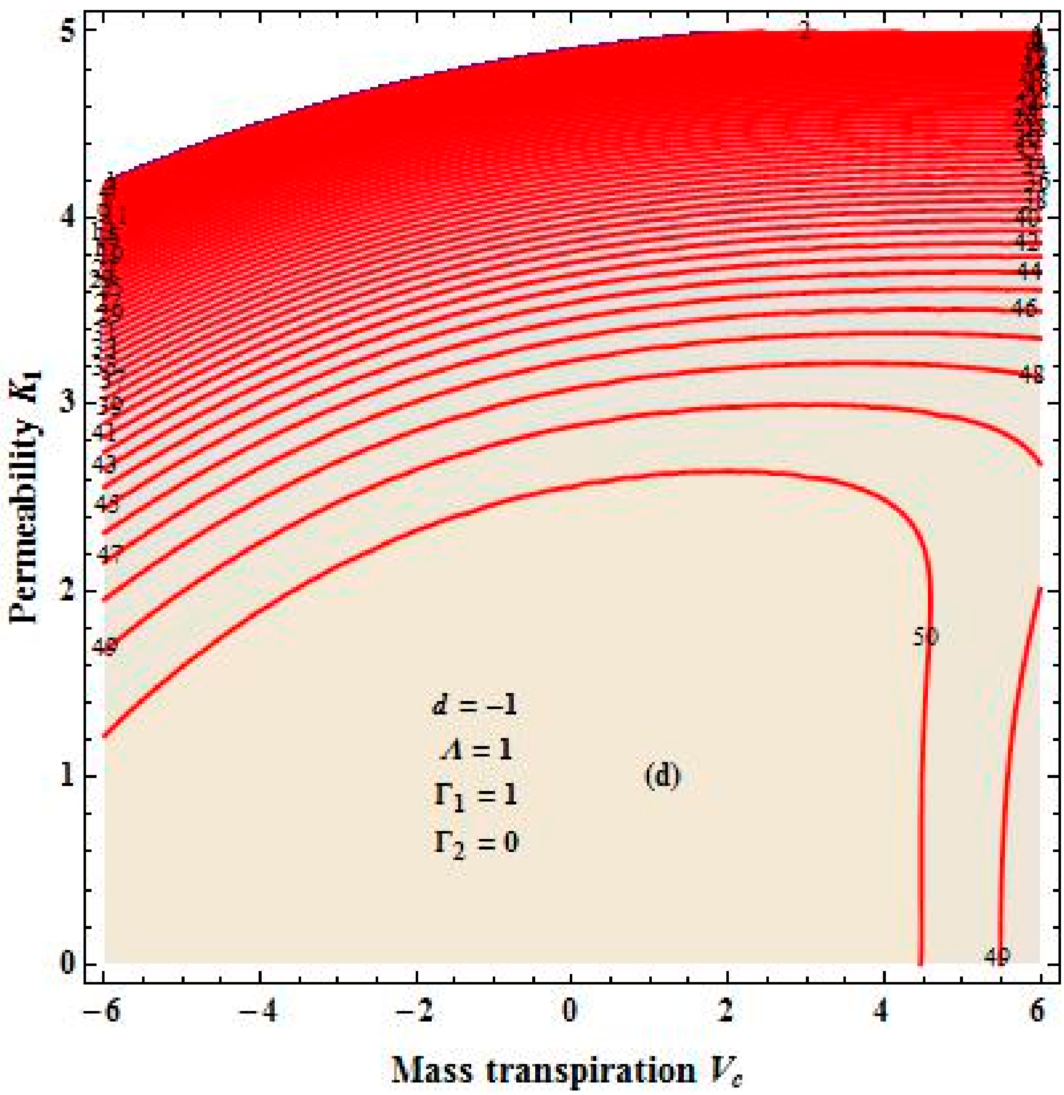

Figure 2. (**a**–**d**) The solution domain of D_1 for K_1 verses mass transpiration V_c with Brinkman ratio $\Lambda = 1$ for the case of a shrinking boundary with different choices of Γ_1 and Γ_2.

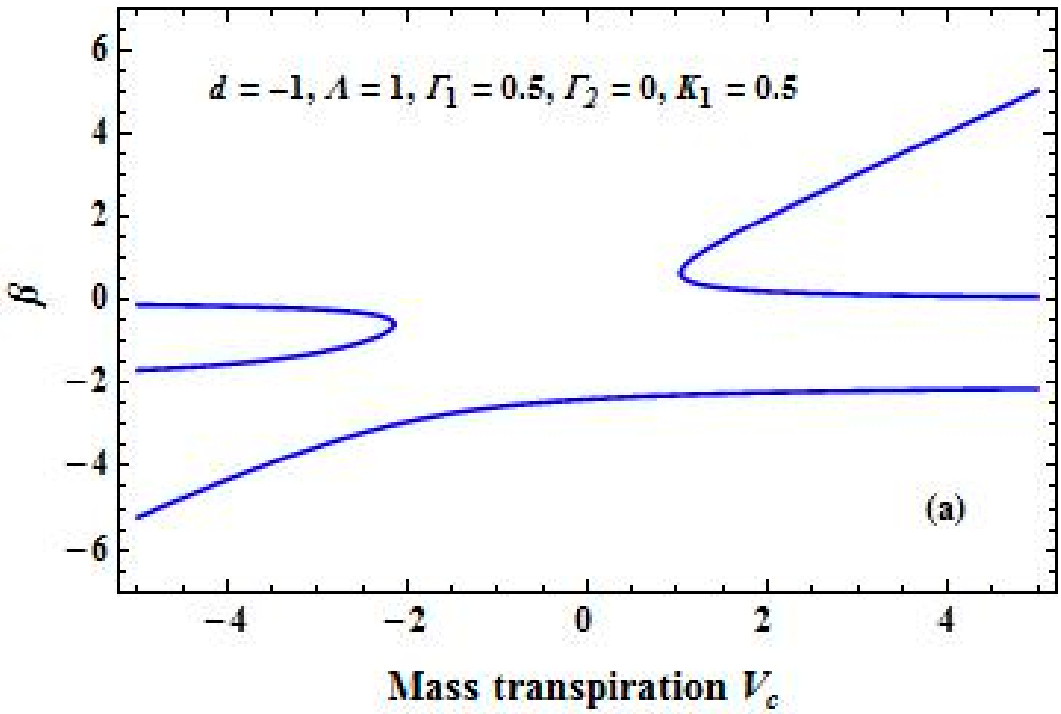

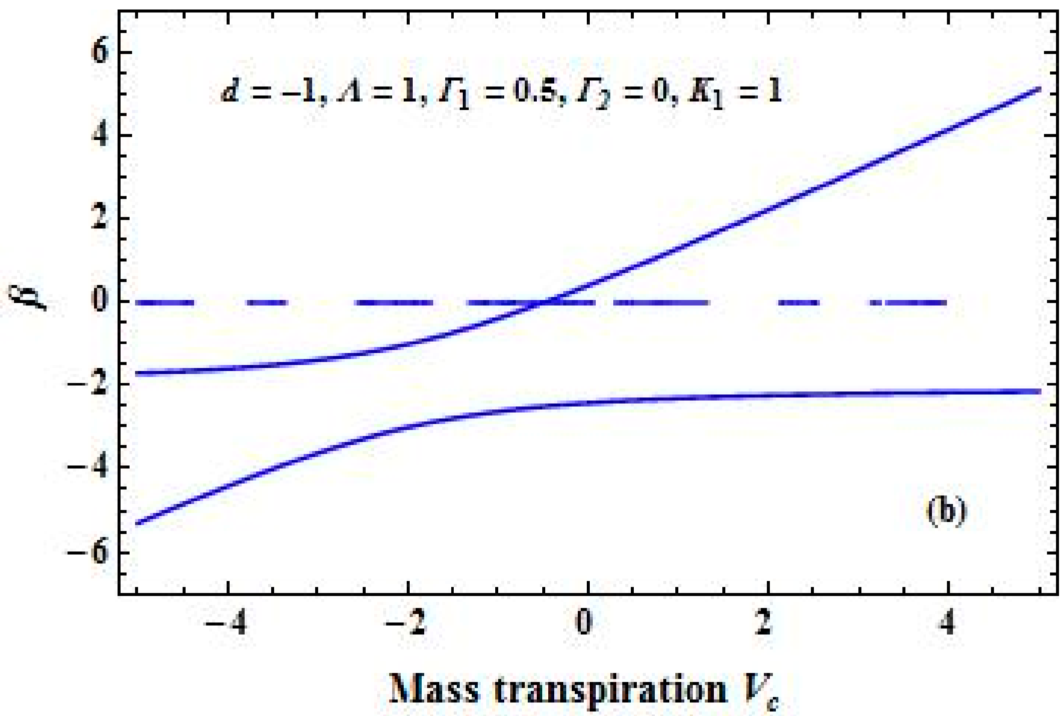

Figure 3. *Cont*.

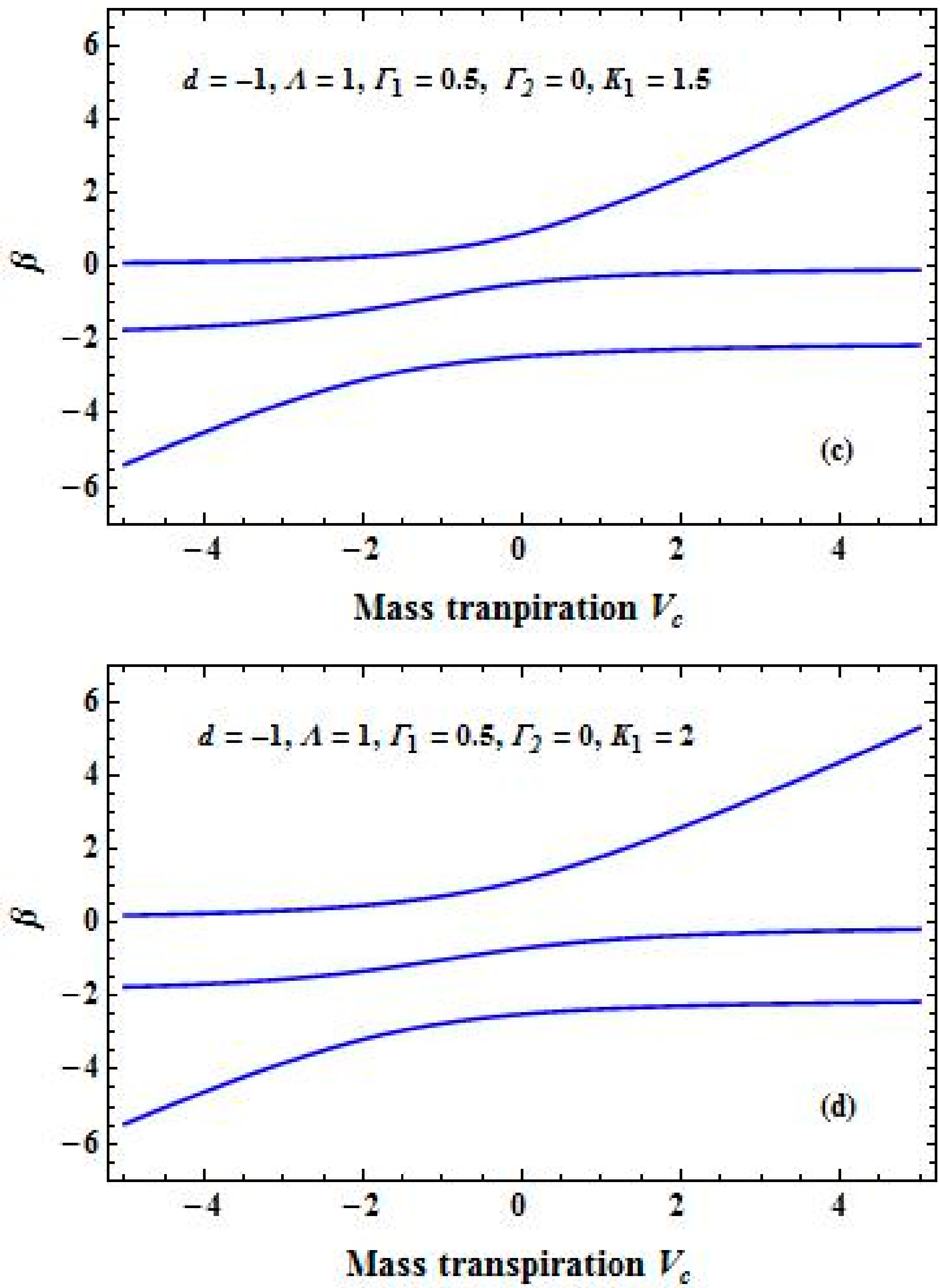

Figure 3. (**a**–**d**) The solution domain of β versus V_c for different values of K_1 for the case of a shrinking boundary.

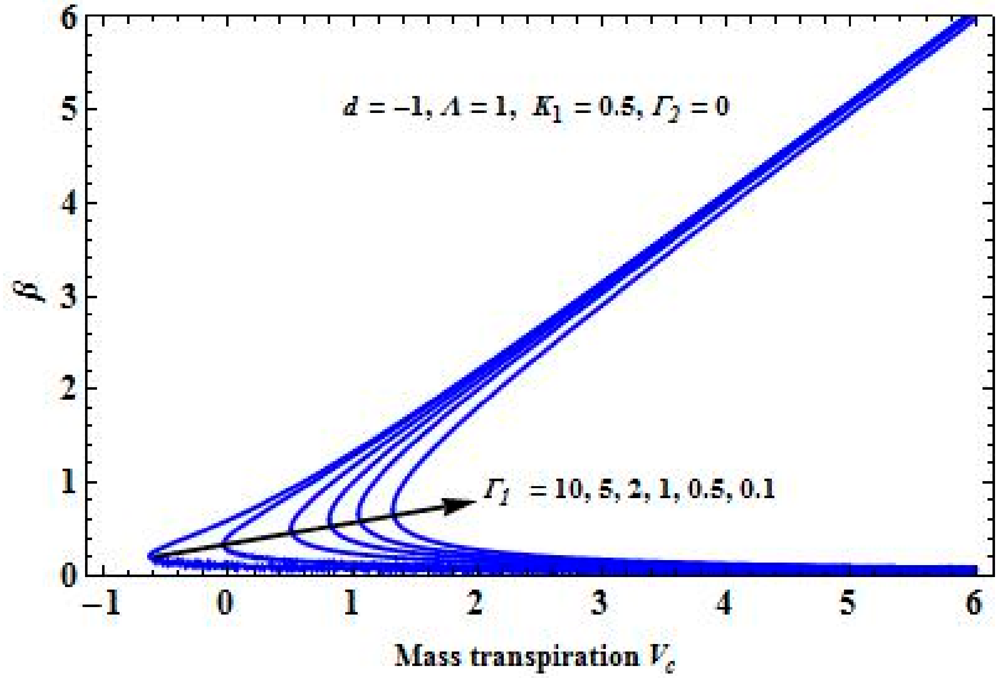

(**a**)

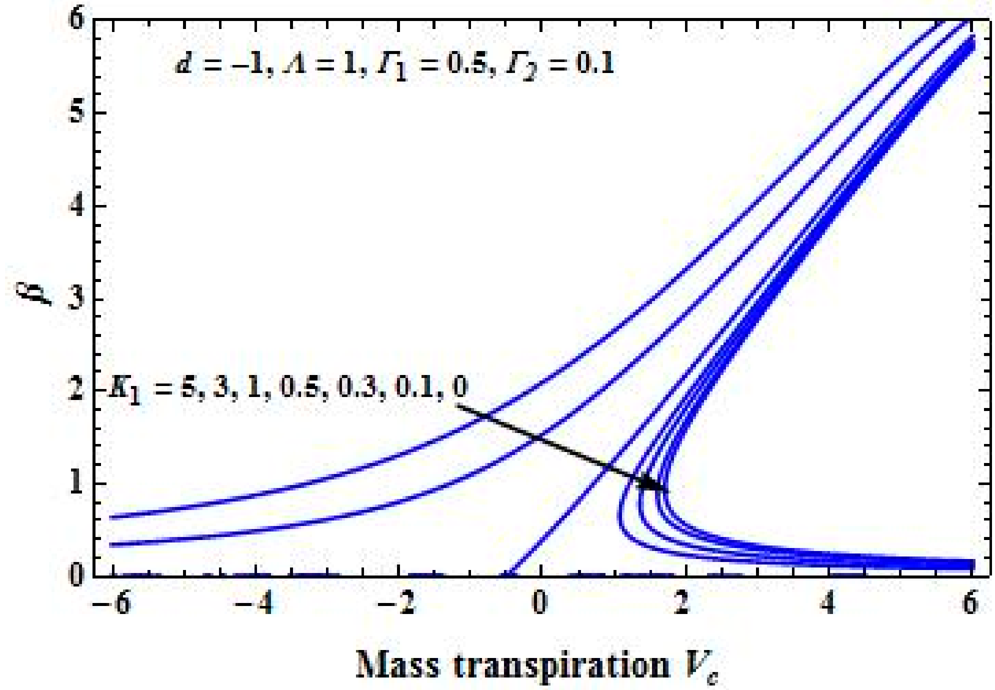

(**b**)

Figure 4. *Cont*.

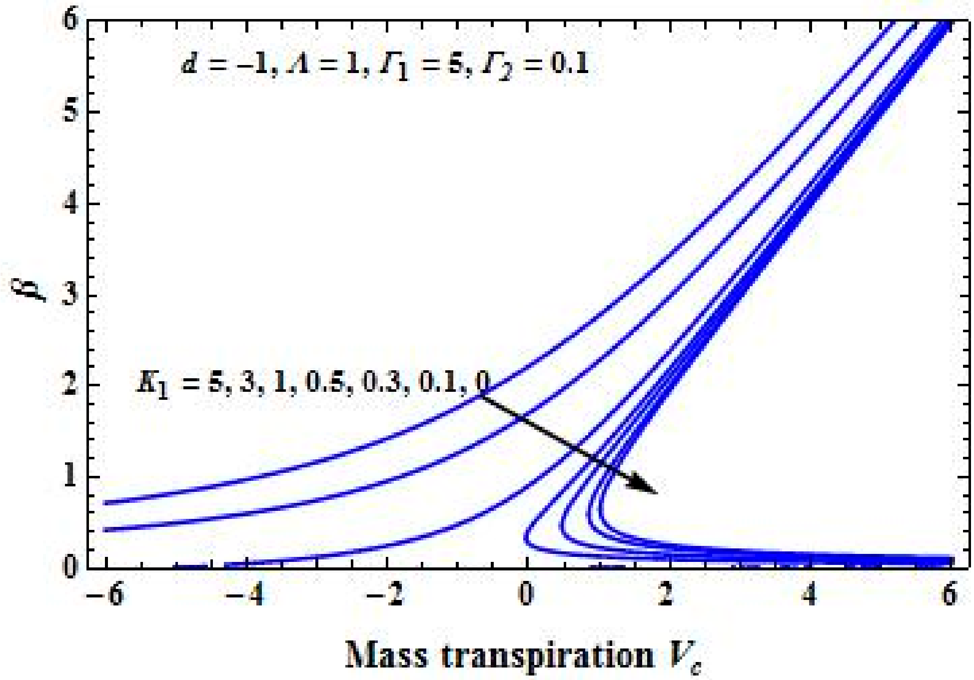

(**c**)

Figure 4. (**a**) The solution domain for β versus V_c for different values of Γ_1 for the case of a shrinking boundary in the absence of Γ_2. (**b**) The solution domain for β versus V_c for different values of K_1 for the case of a shrinking boundary with $\Gamma_1 = 0.5$. (**c**) Solution domain for β versus V_c for different values of K_1 for the case of a shrinking boundary with $\Gamma_1 = 5$.

Figure 5a,b depicts the axial velocity profiles for various values of first-order slip parameters, and for the fixed values of other physical parameters. This plot clearly demonstrates that the increasing Navier's slip results in the reduction of the velocity boundary. In comparison to the lower branch solution, the boundary layer thickness decreases in the case of upper branch solution. Furthermore, under the given slip parameter and mass suction parameter, one can see the increasing velocity boundary thickness with the increase in proportional shearing parameter. Also, the reduction in mass suction leads to the decrease in velocity boundary for other physical parameters fixed. However, for the case of mass injection, the velocity boundary increases with increasing values of slip parameter. Thus, the flow geometry and the rate of change of velocity boundary layer thickness are significantly influenced by the slip parameter.

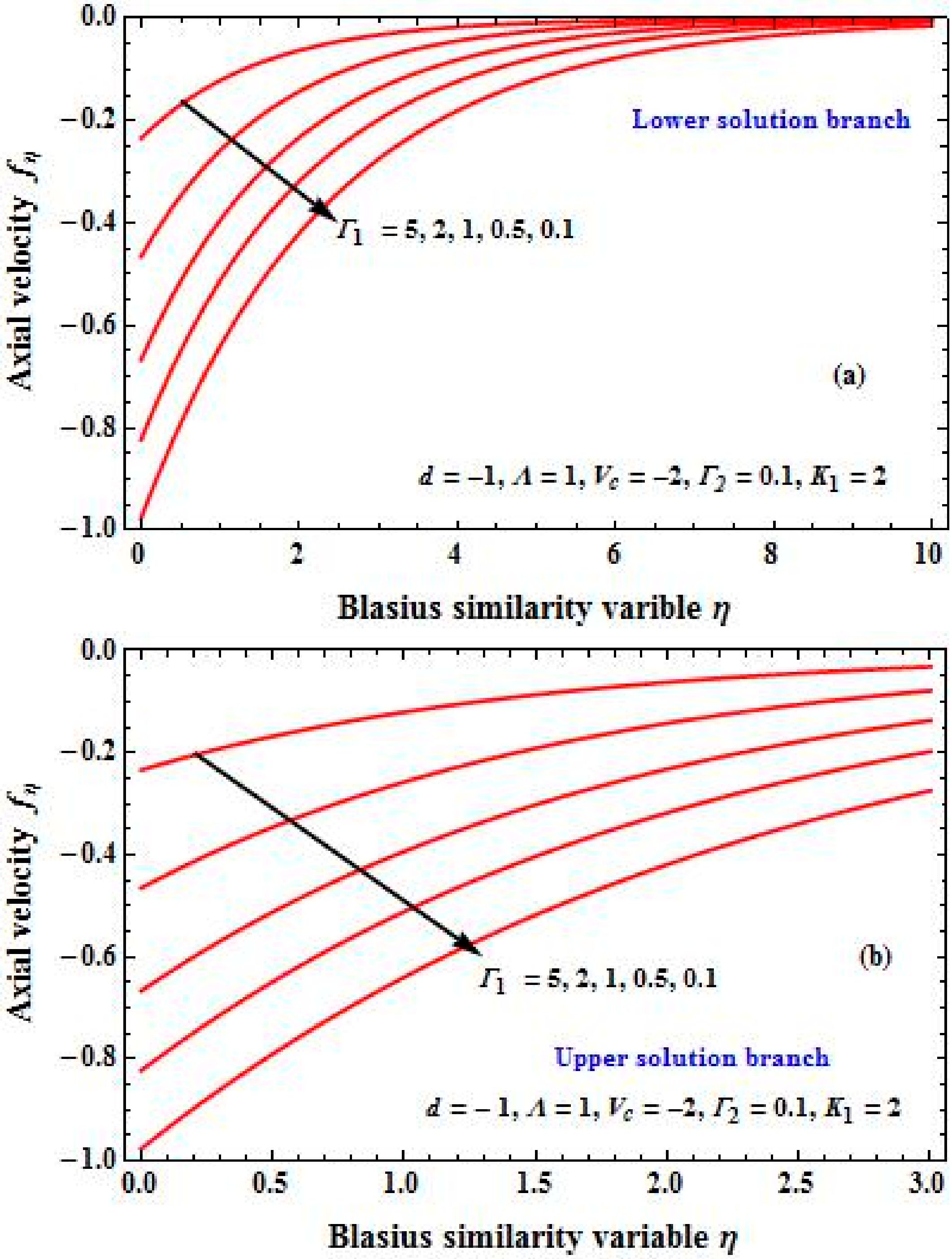

Figure 5. (**a**,**b**) Upper and lower solution branches of axial velocity profile, $f_\eta(\eta)$ verses η, for different values of Navier slip parameter Γ_1 when $K_1 = 0.5$ and $K_1 = 2$ for the case of a shrinking boundary.

Figure 6a–c demonstrates the effect of first- and second-order slip parameters on the axial, as well as transverse velocity profiles respectively, in the accelerating boundary. From the plots, it is clear that the increasing values of first-order slip for fixed values of various physical parameters results in the velocity boundary profiles decreasing, whereas the decreasing value of second-order slip for fixed values of other physical parameters results in the decreasing velocity boundary profiles.

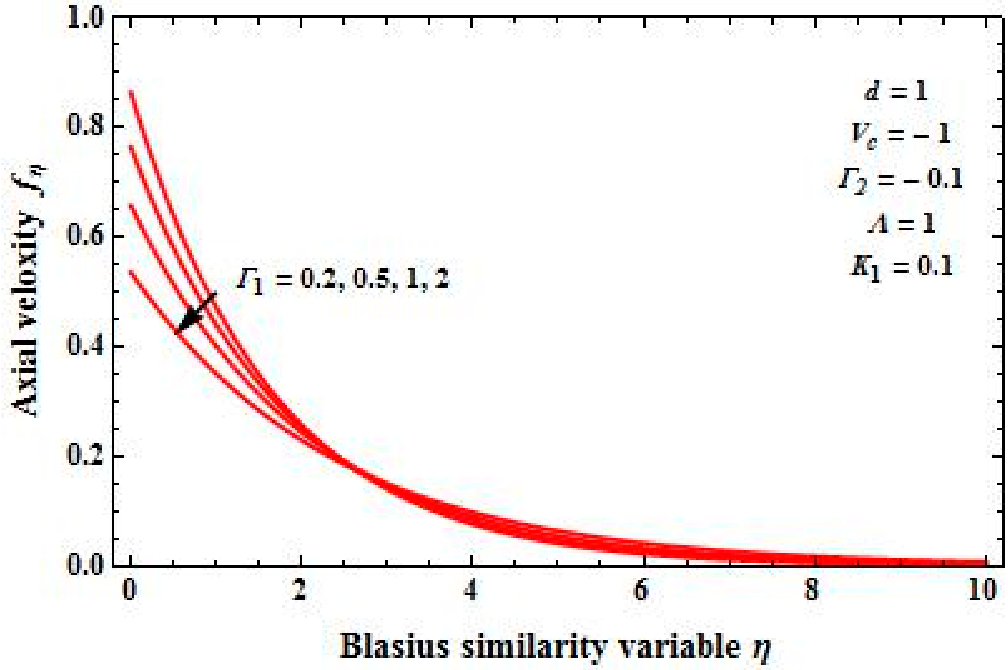

(**a**)

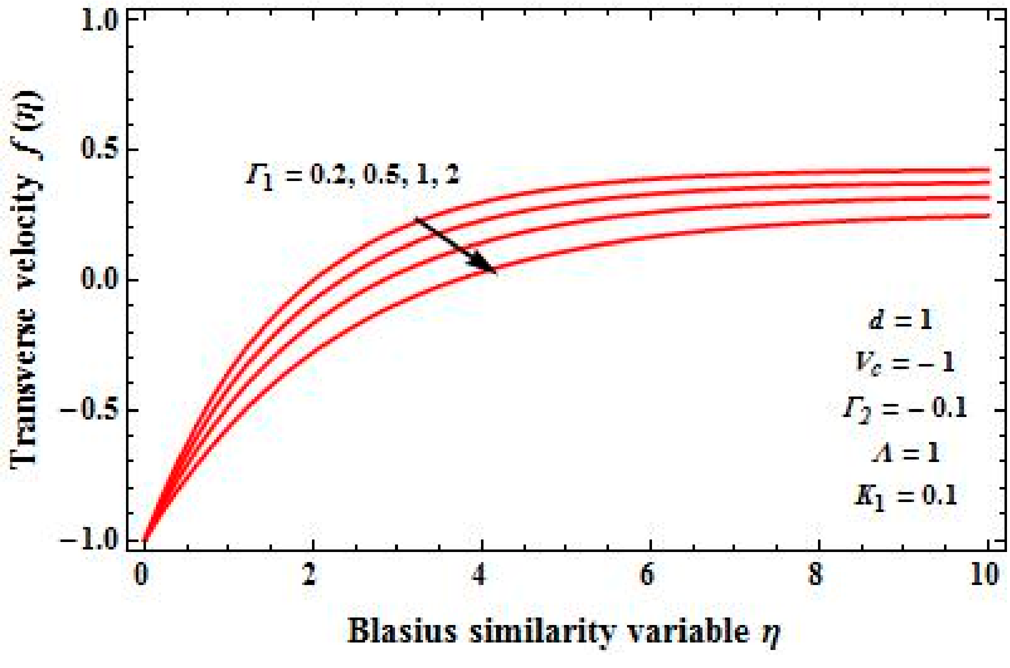

(**b**)

Figure 6. *Cont.*

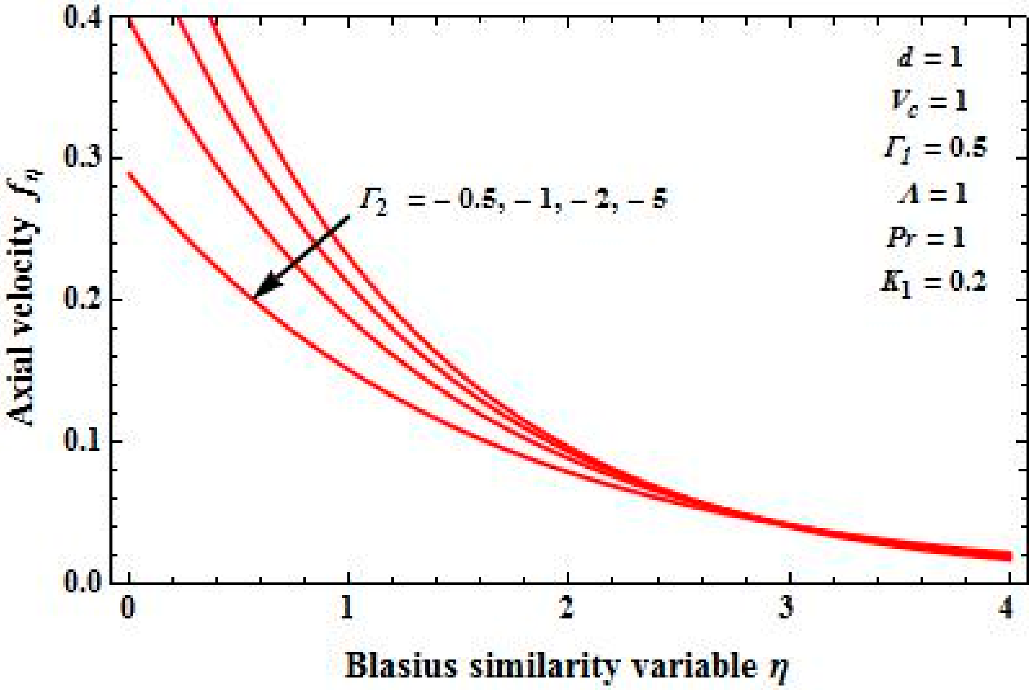

(**c**)

Figure 6. (**a**) Axial velocity $f_\eta(\eta)$ verses η for different values of Γ_1 for the case of a stretching boundary. (**b**) Transverse velocity $f(\eta)$ verses η for different values of Γ_1 with $\Gamma_2 = -0.1$ in the presence of K_1 for the case of a stretching boundary. (**c**) Axial velocity $f_\eta(\eta)$ verses η for different values of Γ_2 with $\Gamma_1 = 0.5$ in the presence of K_1 for the case of a stretching boundary.

Figure 7a,b demonstrates the effect of Brinkman ratio on the axial and transverse velocity profiles. From the plots, it can be seen that increasing values of Λ while keeping other physical parameters fixed results in enhanced boundary layer thickness, whereas in Figure 7c,d, the different values of V_C with fixed Brinkman ratio result in exactly the opposite.

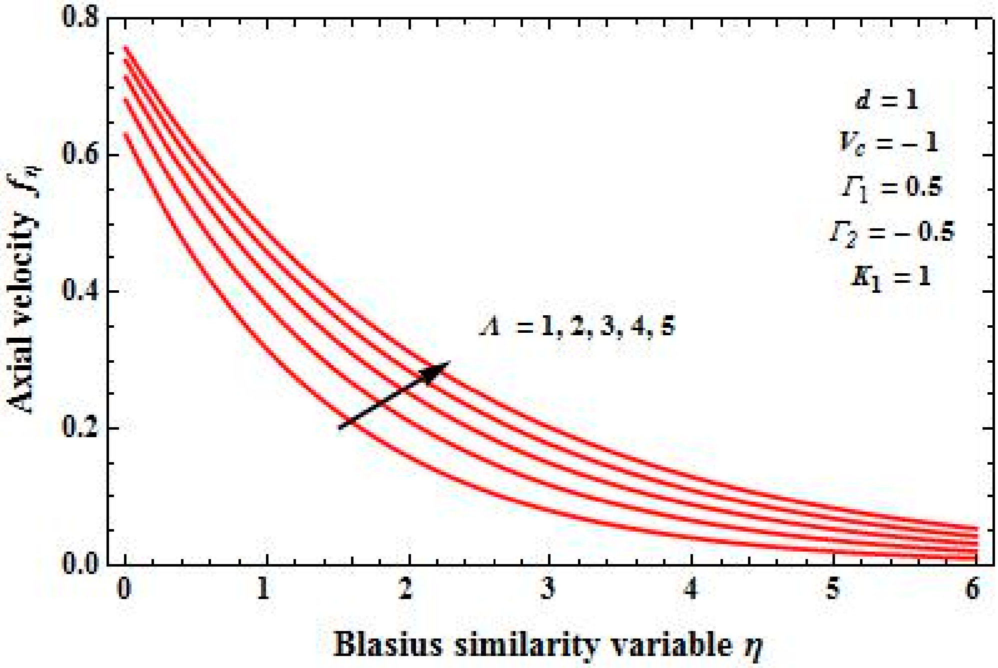

(**a**)

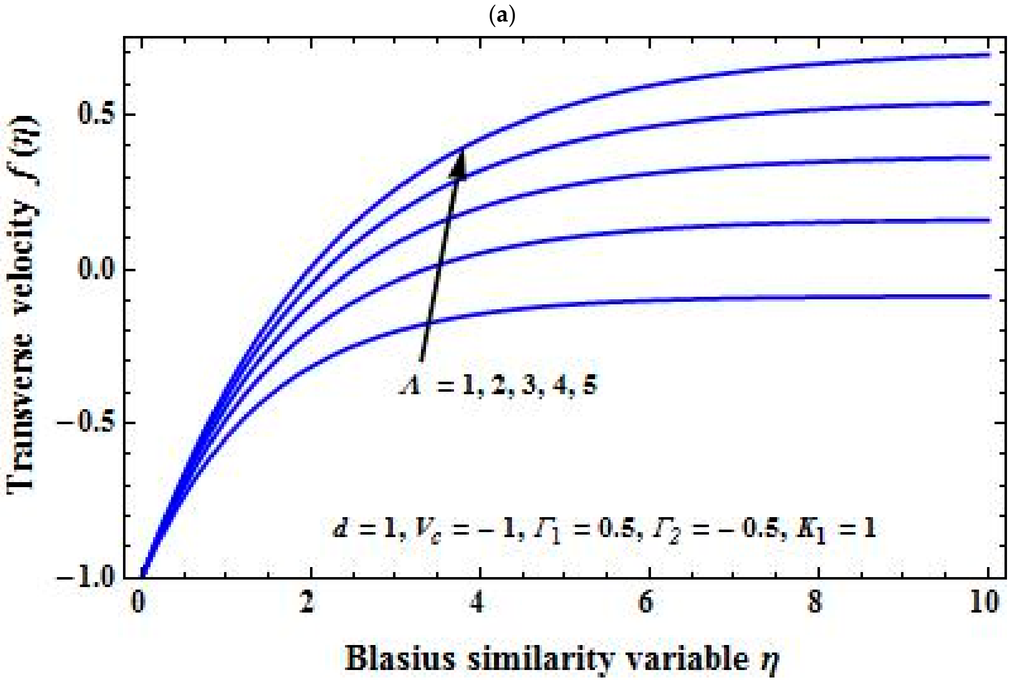

(**b**)

Figure 7. *Cont.*

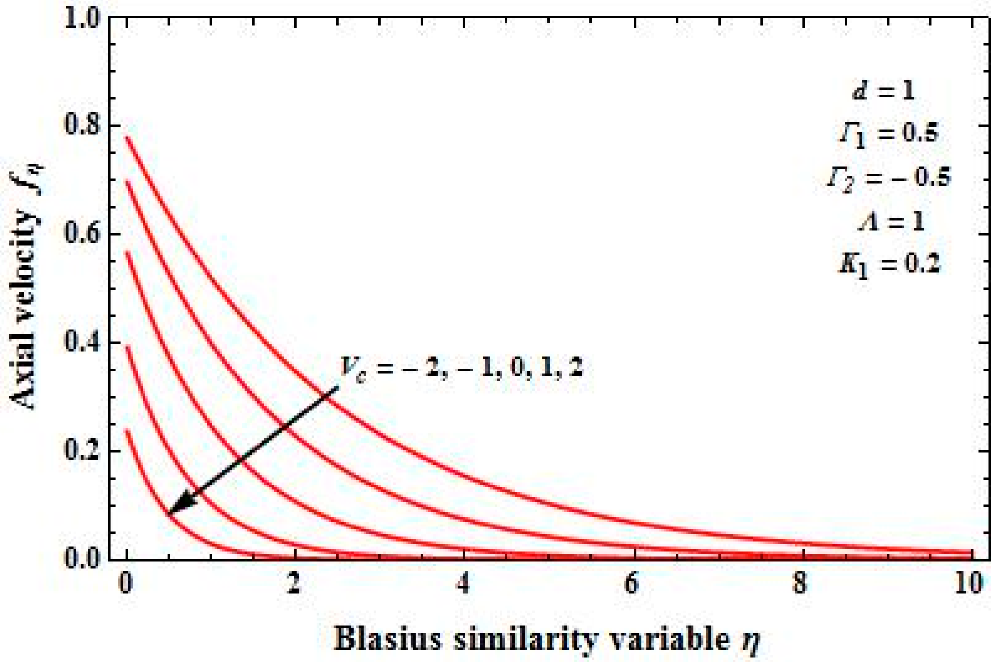

(**c**)

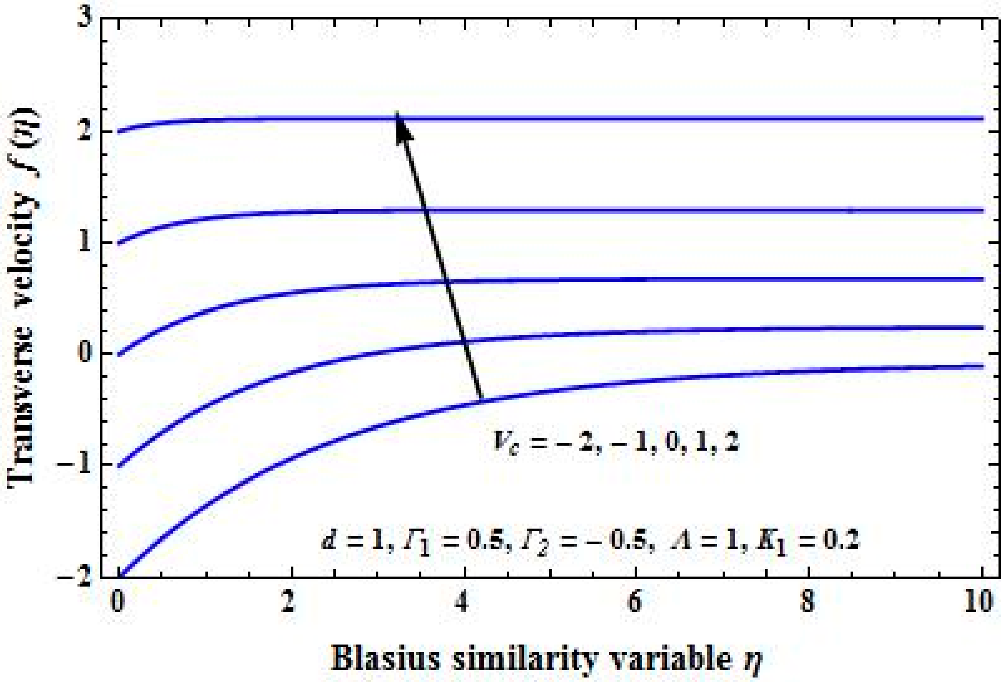

(**d**)

Figure 7. (**a**) Axial velocity $f_\eta(\eta)$ verses η for different values of Λ in the presence of K_1 for the case of a stretching boundary.(**b**) Transverse velocity $f(\eta)$ verses η for different values of Λ in the presence of K_1 for the case of a stretching boundary. (**c**) Axial velocity $f_\eta(\eta)$ verses η for different values of V_c in the presence of K_1 for the case of a stretching boundary. (**d**) Transverse velocity $f(\eta)$ verses η for different values of V_C in the presence of K_1 for the case of the stretching boundary.

Figure 8a,b depicts the effect of various physical parameters on the shear stress profile. In all of these plots, there are crossover points for the shear stress profiles, and the combined effects on the porous solid can be observed. The increase in the values of Γ_1, Γ_2, and K_1 results in increasing shear at the wall boundary. In the case of mass injection, the shear wall boundary decreases faster for a smaller value of second-order slip parameter. Interestingly, however, the increasing value of Brinkman ratio leads to decreasing shear wall boundary as seen in Figure 8a.

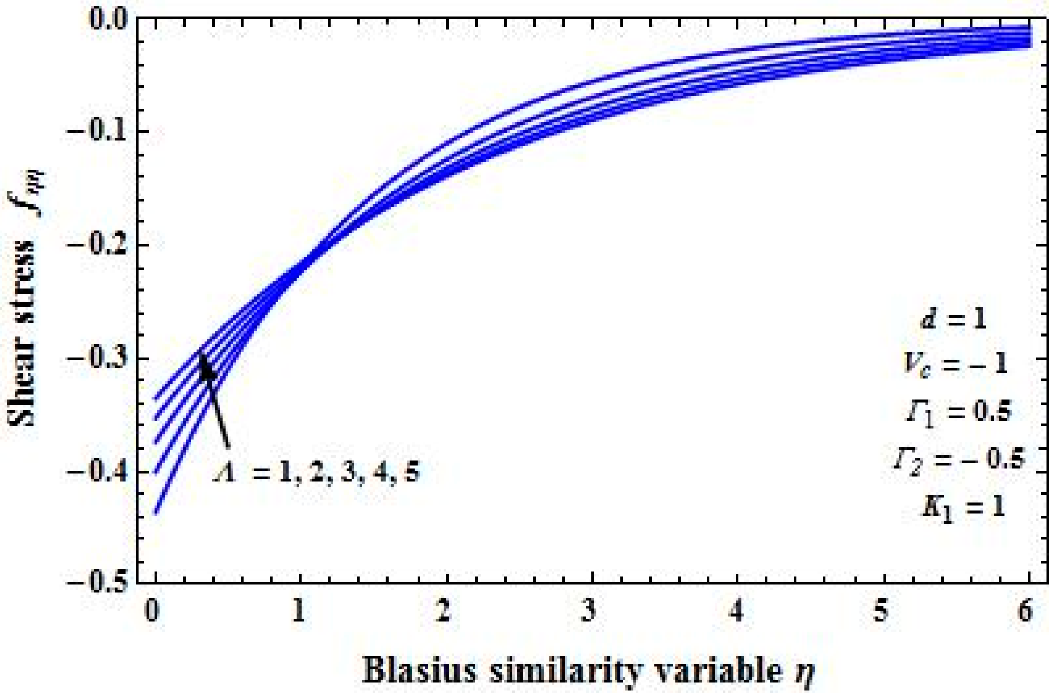

(**a**)

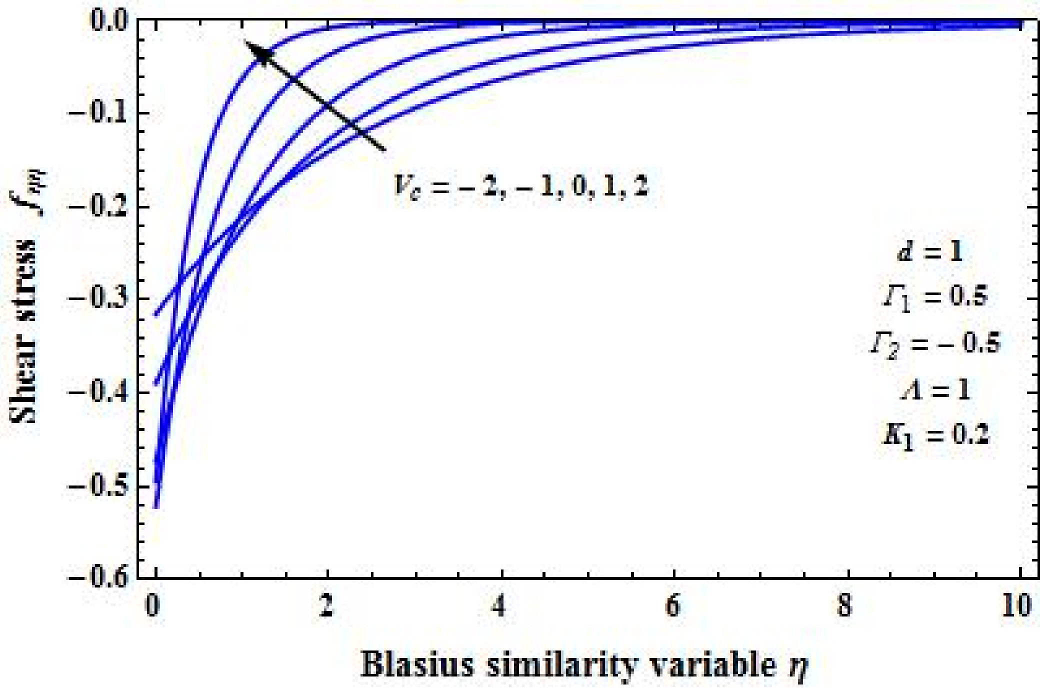

(**b**)

Figure 8. (**a**) Shear stress $f_{\eta\eta}(\eta)$ verses η for different values of Λ in the presence of K_1 for the case of the stretching boundary. (**b**) Shear stress $f_{\eta\eta}(\eta)$ verses η for different values V_c in the presence of K_1 for the case of a stretching boundary.

5. Concluding Remarks

In conclusion, the viscous fluid flow past a porous solid wherein the flow is governed by the Brinkman equation with first- and second-order slip in the presence of mass transpiration was solved, and the exact analytical solution for the governing nonlinear partial differential equation was obtained. The solution was analyzed for the effect of slip parameters, the mass transpiration parameter, the Brinkman ratio, and the extent of shearing or contraction. In the case of the boundary contracting, the solution branches (Figure 5a,b), whereas in the case of the boundary stretching there is only one branch of the solution, and depending on the mass transpiration parameter, the solution is branched (Figure 5a,b).

Author Contributions: Conceptualization, U.S.M., P.N.V.K. and K.R.N.; methodology, U.S.M. and G.B.; software, P.N.V.K., K.R.N., G.B. and S.N.R.N.; validation, G.B; formal analysis, U.S.M., P.N.V.K. and K.R.N.; investigation, K.R.N.; resources, S.N.R.N.; data curation, K.R.N.; writing—original draft preparation, U.S.M., P.N.V.K., K.R.N. and S.N.R.N.; writing—review and editing, P.N.V.K. and G.B.; visualization, G.B. and S.N.R.N.; supervision, U.S.M.; project administration, U.S.M.; funding acquisition, U.S.M.

Funding: This research received no external funding.

Acknowledgments: Author K.R. Nagaraju would like to thank Sri Karisiddappa, Hon'ble Vice-chancellor, VTU, Belagavi, India (Former Principal of Government Engineering College, Hassan-573 201, India) for his valuable support in carrying out his research work.

Conflicts of Interest: The authors declare no conflict of interest.

References

1. Fisher, B.G. *Extrusion of Plastics*, 3rd ed.; Newnes-Butterworld: London, UK, 1976.
2. Brinkman, H.C. On the permeability of the media consisting of closely packed porousparticles. *Appl. Sci. Res.* **1947**, *1*, 81–86. [CrossRef]
3. Darcy, H. *Les Fontaines Publiques De La Ville De Dijon*; Victor Dalmont: Paris, France, 1856.
4. Forchheimer, P. *Wasserbewegung Durch Boden*; Zeitschrift des Vereines Deutscher In-Geneieure: Düsseldorf, Germany, 1901; Volume 45, pp. 1782–1788.
5. Biot, M.A. Mechanics of Deformation and Acoustic Propagation in Porous Media. *J. Appl. Phys.* **1962**, *33*, 1482–1498. [CrossRef]
6. Truesdell, C. Sulla basi della thermomechanical. *Rend. Lincei* **1957**, *22a*, 158–166.
7. Truesdell, C. Sulla basi della thermomechanical. *Rend. Lincei* **1957**, *22b*, 33–38.
8. Chakrabarti, A.; Gupta, A.S. Hydromagnetic flow and heat transfer over a stretching sheet. *Q. Appl. Math.* **1979**, *37*, 73–78. [CrossRef]
9. Gupta, P.S.; Gupta, A.S. Heat and mass transfer on a stretching sheet with suction or blowing. *Can. J. Chem. Eng.* **1977**, *55*, 744–746. [CrossRef]
10. Fang, T. Boundary layer flow over a shrinking sheet with power-law velocity. *Int. J. Heat Mass Transf.* **2008**, *51*, 5838–5843. [CrossRef]
11. Milavcic, M.; Wang, C.Y. Viscous flow due to a shrinking sheet. *Q. Appl. Math.* **2006**, *64*, 283–290. [CrossRef]
12. Nakayama, A. *PC-Aided Numerical Heat Transfer and Convective Flow*; CRC Press: Boca Raton, FL, USA, 1995.
13. Sakiadis, B.C. Boundary-layer behavior on continuous solid surface. *AIChE J.* **1961**, *7*, 26–28. [CrossRef]
14. Sakiadis, B.C. Boundary-layer behavior on continuous solid surfaces. II. The boundary layer on a continuous flat surface. *AIChE J.* **1961**, *7*, 221–225. [CrossRef]
15. Rajagopal, K.R.; Tao, L. *Mechanics of Mixtures*; World Scientific: Singapore, 1995.
16. Givler, R.C.; Altobelli, S.A. A Determination of the Effective Viscosity for the Brinkman-Forchheimer Flow Model. *J. Fluid Mech.* **1994**, *258*, 355–370. [CrossRef]
17. Shao, Q.; Fahs, M.; Hoteit, H.; Carrera, J.; Ackerer, P.; Younes, A. A 3D semi-analytical solution for density-driven flow in porous media. *Water Res. Res.* **2018**, *54*, 10094–10116. [CrossRef]
18. Lesinigo, M.; D'Angelo, C.; Quarteroni, A. A multiscale Darcy-Brinkman model for fluid flow in fractured porous media. *Numer. Math.* **2011**, *117*, 717–752. [CrossRef]
19. Murali, K.; Naidu, V.K.; Venkatesh, B. Solution of Darcy-Brinkman-Forchheimer Equation for Irregular Flow Channel by Finite Elements Approach. *J. Phys. Conf. Ser.* **2019**, *1172*, 012033. [CrossRef]

20. Kumaran, V.; Tamizharasi, R. Pressure in MHD/Brinkman flow past a stretching sheet. *Commun. Nonlinear Sci. Numer. Simul.* **2011**, *16*, 4671–4681.
21. Nield, D.A.; Bejan, A. *Convection in Porous Media*; Springer Verlag Inc.: New York, NY, USA, 1998.
22. Nield, D.A.; Kuznetsov, A.V. Forced convection in porous media: Transverse heterogeneity effects and thermal development. In *Handbook of Porous Media*, 2nd ed.; Vafai, K., Ed.; Taylor and Francis: New York, NY, USA, 2005; pp. 143–193.
23. Nield, D.A. The modeling of viscous dissipation in a saturated porous medium. *J. Heat Transf.* **2007**, *129*, 1459–1463. [CrossRef]
24. Nield, D.A.; Bejan, A. *Convection in Porous Media*, 4th ed.; Springer: New York, NY, USA, 2013.
25. Pantokratoras, A. Flow adjacent to a stretching permeable sheet in a Darcy-Brinkman porous medium. *Transp. Porous Med.* **2009**, *80*, 223–227. [CrossRef]
26. Pop, I.; Ingham, D.B. Flow past a sphere embedded in a porous medium based on the Brinkman model. *Int. Commun. Heat Mass Transf.* **1996**, *23*, 865–874. [CrossRef]
27. Pop, I.; Na, T.Y. A note on MHD flow over a stretching permeable surface. *Mech. Res. Commun.* **1998**, *25*, 263–269. [CrossRef]
28. Pop, I.; Cheng, P. Flow past a circular cylinder embedded in a porous medium based on the Brinkman model. *Int. J. Eng. Sci.* **1992**, *30*, 257–262. [CrossRef]
29. Wang, C.Y. Darcy-Brinkman Flow with Solid Inclusions. *Chem. Eng. Commun.* **2010**, *197*, 261–274. [CrossRef]
30. Srinivasan, S.; Rajagopal, K.R. A thermodynamic basis for the derivation of the Darcy, Forchheimer and Brinkman models for flows through porous media and their generalizations. *Int. J. Non-Linear Mech.* **2014**, *58*, 162–166. [CrossRef]
31. Ingham, D.B.; Pop, I. *Transport in Porous Media*; Pergamon: Oxford, UK, 2002.
32. Magyari, E.; Keller, B. Exact solutions for self-similar boundary-layer flows induced by permeable stretching surfaces. *Eur. J. Mech. B* **2000**, *19*, 109–122. [CrossRef]
33. Mastroberardino, A.; Mahabaleshwar, U.S. Mixed convection in viscoelastic flow due to a stretching sheet in a porous medium. *J. Porous Media* **2013**, *16*, 483–500. [CrossRef]
34. Siddheshwar, P.G.; Mahabaleshwar, U.S. Effects of radiation and heat source on MHD flow of a viscoelastic liquid and heat transfer over a stretching sheet. *Int. J. Non-Linear Mech.* **2005**, *40*, 807–820. [CrossRef]
35. Siddheshwar, P.G.; Chan, A.; Mahabaleshwar, U.S. Suction-induced magnetohydrodynamics of a viscoelastic fluid over a stretching surface within a porous medium. *IMA J. Appl. Math.* **2014**, *79*, 445–458. [CrossRef]
36. Tamayol, A.; Hooman, K.; Bahrami, M. Thermal analysis of flow in a porous medium over a permeable stretching wall. *Transp. Porous Media* **2010**, *85*, 661–676. [CrossRef]
37. Shao, Q.; Fahs, M.; Younes, A.; Makradi, A. A High Accurate Solution for Darcy-Brinkman Double-Diffusive Convection in Saturated Porous Media. *J. Numer. Heat Transf. Part B Fundam.* **2015**, *69*, 26–47. [CrossRef]
38. Navier, C.L.M.H. Mémoire sur les lois du mouvement des fluids. *Mém. Acad. R. Sci. Inst. Fr.* **1827**, *6*, 389–440.
39. Brinkman, H.C. A calculation of the viscous force exerted by a flowing fluid on a dense swarm of particles. *Appl. Sci. Res.* **1949**, *1*, 27–34. [CrossRef]
40. Mahabaleshwar, U.S.; Nagaraju, K.R.; Kumar, P.N.V.; Baleanu, D.; Lorenzini, G. An exact analytical solution of the unsteady magnetohydrodynamics nonlinear dynamics of laminar boundary layer due to an impulsively linear stretching sheet. *Contin. Mech. Thermodyn.* **2017**, *29*, 559–567. [CrossRef]
41. Rajagopal, K.R. On a hierarchy of approximate models for flows of incompressible fluids through porous solids. *Math. Model. Methods Appl. Sci.* **2007**, *17*, 215–252. [CrossRef]
42. Vafai, K.; Tien, C.L. Boundary and inertia effects on flow and heat transfer in porous media. *Int. J. Heat Mass Transf.* **1981**, *24*, 195–203. [CrossRef]
43. Fang, T.; Aziz, A. Viscous flow with second-order slip velocity over a stretching sheet. *Zeitschrift Für Naturforschung A* **2010**, *65*, 1087–1092. [CrossRef]
44. Lin, W. Mass transfer induced slip effect on viscous gas flows above a shrinking/stretching sheet. *Int. J. Heat Mass Transf.* **2016**, *93*, 17–22.
45. Andersson, H.I. Slip flow past a stretching surface. *Acta Mech.* **2002**, *158*, 121–125. [CrossRef]
46. Crane, L.J. Flow past a stretching plate. *Z. Angew. Math. Phys.* **1970**, *21*, 645–647. [CrossRef]
47. Pavlov, K.B. Magnetohydrodynamic flow of an incompressible viscous liquid caused by deformation of plane surface. *Magn. Gidrodin.* **1974**, *4*, 146–147.

48. Wang, C.Y. Flow due to a stretching boundary with partial slip—An exact solution of the Navier-Stokes equations. *Chem. Eng. Sci.* **2002**, *57*, 3745–3747. [CrossRef]
49. Abramowitz, M.; Stegun, I.A. *Handbook of Mathematical Functions with Formulas, Graphs, and Mathematical Tables*, 9th ed.; Dover: New York, NY, USA, 1972; pp. 17–18.
50. Birkhoff, G.; MacLane, S. *A Survey of Modern Algebra*; Macmillan: New York, NY, USA, 1996; pp. 107–108.
51. Fang, T.-G.; Zhang, J.; Yao, S.-S. Slip Magnetohydrodynamic Viscous Flow over a Permeable Shrinking Sheet. *Chin. Phys. Lett.* **2010**, *27*, 124702. [CrossRef]
52. Fang, T.; Yao, S.; Zhang, J.; Aziz, A. Viscous flow over a shrinking sheet with a second order slip flow model. *Commun. Nonlinear Sci. Numer. Simul.* **2010**, *15*, 1831–1842. [CrossRef]